

expect the projection-operator method will provide an economical way to arrive at exact equations which allow a direct physical interpretation of all terms without the presence of complicated modified propagators present in the projection-operator

analysis of more realistic systems.

#### ACKNOWLEDGMENT

We would like to thank Professor I. Oppenheim for stimulating discussions.

\*Work supported by the National Science Foundation.

<sup>†</sup>Alfred P. Sloan Fellows.

<sup>1</sup>J. Lebowitz and P. Resibois, *Phys. Rev.* **139**, A1101 (1965), and references cited therein.

<sup>2</sup>H. Mori, *Progr. Theoret. Phys. (Kyoto)* **33**, 423 (1965).

<sup>3</sup>P. Mazur and I. Oppenheim, *J. Phys. Soc. Japan Suppl.* **26**, 35 (1969).

<sup>4</sup>R. J. Rubin, *Phys. Rev.* **131**, 964 (1963). Professor Zwanzig has studied (unpublished notes) Rubin's model in great detail using a projection operator entirely different from the two discussed here.

<sup>5</sup>P. Mazur and E. Montroll, *J. Math. Phys.* **1**, 70 (1960); G. W. Ford, M. Kac, and P. Mazur, *ibid.* **6**, 504 (1965).

<sup>6</sup>P. Ullersma, *Physica* **32**, 27 (1966); **32**, 56 (1966); **32**, 74 (1966).

<sup>7</sup>P. Mazur and E. Braun, *Physica* **30**, 1973 (1964).

<sup>8</sup>M. Toda, *J. Phys. Soc. Japan* **14**, 722 (1959).

<sup>9</sup>I. Oppenheim and P. Mazur, *Physica* (to be published).

<sup>10</sup>For a discussion of projection-operator techniques to describe two Brownian particles in a general fluid, see J. M. Deutch and I. Oppenheim, *J. Chem. Phys.* (to be published).

PHYSICAL REVIEW A

VOLUME 3, NUMBER 6

JUNE 1971

## Thermomagnetic Force in Polyatomic Gases\*

M. E. Larchez<sup>†</sup> and T. W. Adair, III

*Texas A & M University, College Station, Texas 77843*

(Received 28 December 1970)

A force has been observed on a small thin disk which is immersed in a polyatomic gas when a thermal gradient is established and when a magnetic field is applied. This thermomagnetic force is normal to the surface of the disk and is an even function of the magnetic field. Measurements are reported of this force effect as a function of magnetic field and pressure for O<sub>2</sub> and NO in the temperature range 30–35°C. These new results are compared to a related thermomagnetic effect on the thermal conductivity of a polyatomic gas (Sentrleben-Beenakker effect).

### I. INTRODUCTION

It has been known for forty years that a magnetic field could influence the transport properties of some gases. The first observation of such an influence was made when it was discovered that a magnetic field causes a decrease in the thermal conductivity of oxygen.<sup>1</sup> Two years later it was discovered that a magnetic field also causes a decrease in the shear viscosity of oxygen.<sup>2</sup> These effects in O<sub>2</sub> were later observed in NO and were extensively studied. It was observed that the transport coefficients decrease in a magnetic field  $H$ , that the effect is an even function of  $H$ , and that the effect approaches saturation as a function of field divided by pressure  $H/P$ .

All of the measurements can be explained qualitatively in terms of a model in which a rotating diatomic molecule of O<sub>2</sub> is considered as a disk with a magnetic moment in the direction of the axis of rotation.<sup>3,4</sup> Each disk clearly has a lower probability of a collision when moving in its own plane than when moving perpendicular to it; equivalently, a disk has a lower collision probability when the velocity and the rotational angular momentum vectors are perpendicular than when they

are parallel. In the absence of an external magnetic field this causes no observable asymmetry in the properties of the gas because the velocities and angular momenta are randomly oriented and the asymmetries are averaged out. When a magnetic field is applied the averaging out is partially destroyed by the precession of the angular momenta about the field. The way this leads to a change in measurable properties of the gas can easily be imagined, for example, by picturing a molecule whose angular momentum and magnetic moment are perpendicular to the field. If the field and the magnetic moment are large enough to cause substantial precession between collisions, the disk presents a more nearly spherical collision cross section and the possibility of relatively unimpeded motion in the plane of the disk is lost. Upon averaging over all orientations of velocity and angular momentum of the molecules, the result is that the change in collision cross section causes, on the whole, a reduction in the thermal conductivity and the viscosity. Since these effects were thought to be only properties of strongly paramagnetic gases (the only ones studied) and since the Gorter<sup>3</sup> model explained the measurements reasonably well, interest diminished.

The model discussed above predicts the same magnetic effects on the transport properties of polyatomic molecules which have rotational magnetic moments. These rotational magnetic moments are small (the order of nuclear moments) and thus the magnetic fields necessary to cause sufficient precession of the molecules are considerably larger than those necessary for  $O_2$  and  $NO$ . The influence of the magnetic field on the transport properties of  $N_2$  and other polyatomic molecules was experimentally verified by Beenakker *et al.*<sup>5</sup> This discovery, along with advances in the kinetic theory of transport, revived interest in these magnetic effects. Since then extensive investigations have been conducted on these field effects [now called Senftleben-Beenakker (SB) effects] in numerous gases. A comprehensive review and bibliography of the experimental and theoretical work in this field can be found in the review articles by Beenakker<sup>6</sup> and Beenakker and McCourt.<sup>7</sup>

The most recently discovered manifestation of the effect of a magnetic field on polyatomic molecular interactions is the thermomagnetic torque known as the Scott effect.<sup>8</sup> When a small cylinder is suspended as a torsion pendulum in a polyatomic gas, and a radial thermal gradient is established between the cylinder and the surrounding gas, the application of a vertical magnetic field causes a torque on the cylinder. If the magnetic field or the thermal gradient is reversed the torque will reverse. Also, the direction of the torque depends on the sign of the gyromagnetic ratio of the molecules. The torque is small but  $10^7$  times too large to be explained by the direct exchange of angular momentum between the molecules and the surface of the cylinder. This thermomagnetic torque is neither observed in gases of spherical molecules with zero magnetic moment, like argon and helium, nor in gases of spherical molecules with nonzero magnetic moment like  $^3He$ .<sup>9</sup>

The understanding of a Scott torque acting on a torsion pendulum requires a collision process between molecules which results in a net toroidal flow of the gas at the pendulum surface.<sup>10,11</sup> Gas collisions with the surface of the pendulum produce a net steady torque. A review of the experi-

mental and theoretical work on the Scott torque along with a bibliography may be found in the paper by Beenakker and McCourt.<sup>7</sup>

We report here measurements of a new and different thermomagnetic effect which we hope may give further understanding of the same molecular collision processes. This effect is a magnetic-field-induced change in the radiometer force which a polyatomic gas exerts normal to the surface on which it acts when a thermal gradient exists at the surface. Details are presented in Secs. II-IV.

## II. EXPERIMENTAL APPARATUS

The apparatus that was used to measure the thermomagnetic force is shown schematically in Fig. 1. An aluminum disk  $D$  22.2 mm in diam and 0.02 mm thick was suspended by a quartz fiber  $Q$  2.5 mm above a flat copper plate  $HP$ . The disk and fiber were suspended by a sensitive quartz spring  $S$ . An extension or compression of the spring corresponding to a force of  $3 \times 10^{-4}$  dyn could be measured with the micrometer microscope  $M$ . A thermal gradient was established by heating the copper plate with a 1-W wire heater wound around the copper plate. The temperature of this hot plate was measured by a copper constantan thermocouple  $T$  placed on the surface. The temperature of the aluminum sensing disk was obtained by measuring the temperature of a small disk placed at the same height as the sensing disk. All measurements were made with the sensing disk at a temperature of between 30-35 °C and the temperature difference between this sensing disk and the copper plate was 1-2 °C. The major inaccuracy in the temperature was due to assuming the temperature of the small disk was the same as the temperature of the sensing disk. In order to be able to estimate the accuracy of this assumption, a thermocouple was placed on the sensing disk. Measurements were made of the temperature of the sensing disk and of the small disk at various temperatures. These measurements indicated that the temperatures which were used for the sensing disk were within  $\pm 0.3$  °C of the actual temperature.

Two different pairs of Helmholtz coils were used to produce the magnetic field. For the smaller fields, a large pair of coils was used which had an inner diameter of 60 cm and an outer diameter of 68 cm. A small set of Helmholtz coils was used for the higher fields. These coils were 15 cm i.d. and 32 cm o.d. The horizontal and vertical components of the Earth's magnetic field were canceled by independent Helmholtz coils. All magnetic fields were measured with a Rawson Model 726 rotating coil gaussmeter. Gas pressure in the system was measured to an accuracy of  $\pm 5 \mu$  with an oil manometer and cathetometer.

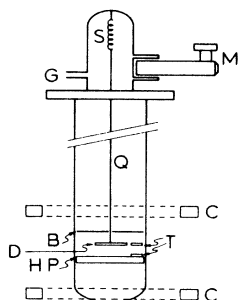


FIG. 1. Schematic diagram of equipment.  $D$ , sensing disk;  $HP$ , hot plate;  $T$ , thermocouples;  $B$ , baffle;  $C$ , Helmholtz coils;  $Q$ , quartz support fiber;  $S$ , spring;  $M$ , microscope; and  $G$ , filling line.

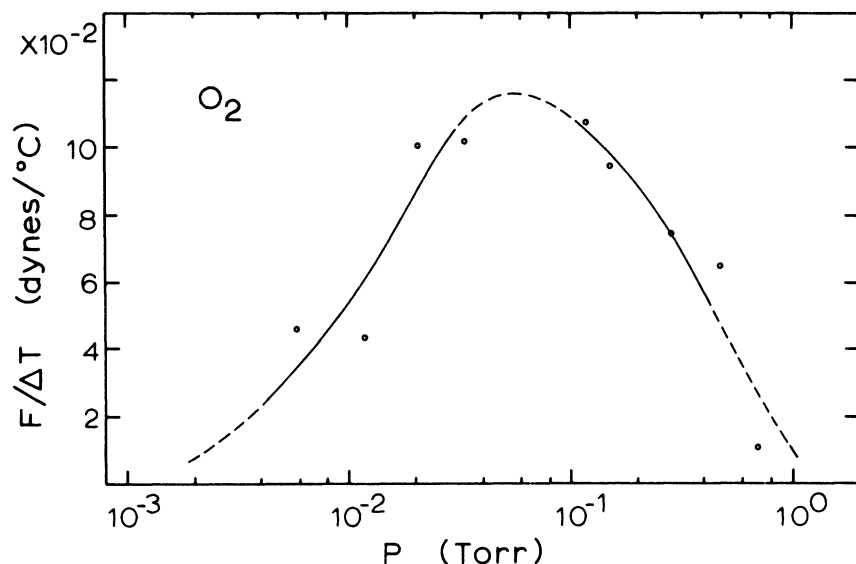


FIG. 2. Field-free force normalized to  $\Delta T = 1^\circ\text{C}$  as a function of pressure in  $\text{O}_2$  (log scale).

The oxygen used in these experiments was obtained from AIRCO and the nitric oxide from Matheson Gas Products. The stated purity of the  $\text{O}_2$  was 99.99% and that of the NO was 98.5%.

### III. EXPERIMENTAL RESULTS

When a thermal gradient is established by heating the copper plate a steady-state upward radiometer-type force<sup>12,13</sup> is exerted by a gas on the sensing disk. Thus far we consider only zero magnetic field. Measurements of this field-free force as a function of the pressure for oxygen are shown in Fig. 2. Note that the force is shown as force per degree, that is, normalized to one degree difference between the temperature of the heater plate and that of the plate adjacent to the force sensing disk. The scatter in the data is due to the uncertainty in the temperature. The force on the disk has the same pressure dependence as does the radiometer force<sup>12</sup>:

$$F = (a/p + b)^{-1}, \quad (1)$$

where  $a$  and  $b$  are empirically determined constants. The maximum of the field-free force occurs at a pressure of 0.05 Torr, which is also the pressure for the maximum radiometer force.

The thermomagnetic force is a downward force about two orders of magnitude smaller than the field-free force and is measured as a change in the force on the disk. This force is an even function of  $H$ .

A value for the thermomagnetic force at each pressure and field is obtained by measuring the extension of the quartz spring as the field is turned on up and then down. The extension of the spring in zero field is carefully measured before and after each field measurement. A typical series

of four such measurements in a period of 20–30 min yields one data point. Pressure measurements before and after the series of force measurements indicate that there is no measurable pressure drift. This is also confirmed by the constant values of the zero-field force obtained during the measurements.

The thermomagnetic force normalized to  $\Delta T = 1^\circ\text{C}$  as a function of  $H$  is shown in Fig. 3 for oxygen at pressures 0.10, 0.19, 0.26, and 0.36 Torr with the field directed vertically (parallel to the temperature gradient). For all pressures the force increases with increasing  $H$  up to a maximum at about  $H = 100$  Oe. The maximum normalized force is about  $10^{-3}$  dyn/ $^\circ\text{C}$ , which is roughly 1% of the field-free force of Fig. 2.

Figure 4 is a plot of the same data as that of Fig. 3 but the force, normalized to  $\Delta T = 1^\circ\text{C}$ , is shown as a function of the field-to-pressure ratio  $H/P$ . The force increases as  $H/P$  increases and reaches a maximum at about  $H/P = 600$  Oe/Torr. In the region where the force is increasing with  $H/P$  the points fall more nearly along a single curve than they did in Fig. 3, indicating that in that region the effect is a function of  $H/P$ . However, at the larger values of  $H/P$  it is not evident that this  $H/P$  dependence holds. The position of the curve on the  $H/P$  axis can be specified by the value of  $H/P$  for which the normalized force has half of its maximum value, called the half-value  $(H/P)_{1/2}$ , and this value from Fig. 4 for  $\text{O}_2$  with vertical field is  $(H/P)_{1/2} = 10 \pm 1$  Oe/Torr.

In Fig. 5, the normalized force is plotted as a function of  $H/P$  for  $\text{O}_2$  with the magnetic field horizontal (perpendicular to the temperature gradient). Pressures were the same for these measurements as for those of Fig. 3. These data points for

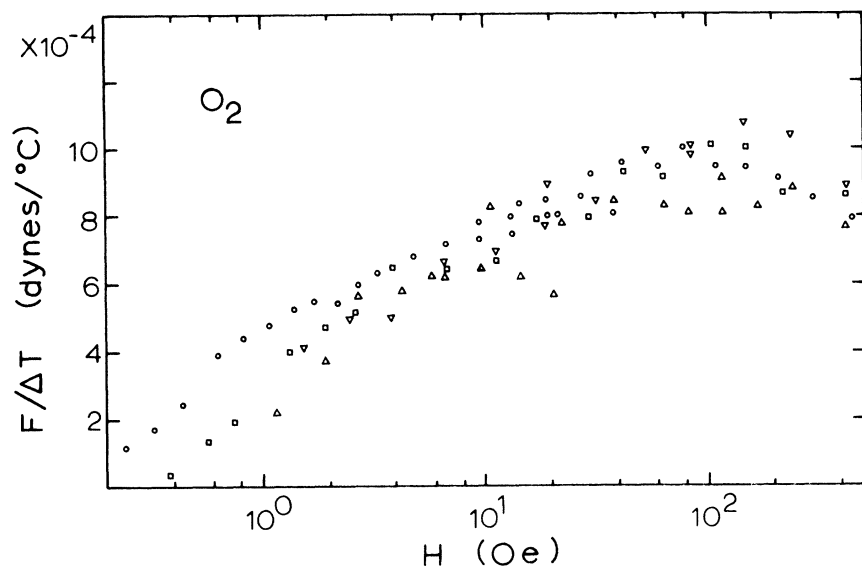


FIG. 3. Thermomagnetic force in  $O_2$  normalized to  $\Delta T = 1^\circ C$  as a function of magnetic field with field parallel to thermal gradient (log scale).  $\circ$ ,  $P = 0.10$  Torr;  $\square$ ,  $P = 0.19$  Torr;  $\nabla$ ,  $P = 0.26$  Torr;  $\Delta$ ,  $P = 0.36$  Torr.

horizontal field also lie along a single curve as the force increases with increasing  $H/P$ . The maximum value of the normalized force is approximately  $12 \times 10^{-4} \text{ dyn}/^\circ C$ , which is slightly larger than the value obtained with the field vertical. The  $(H/P)_{1/2}$  value for the horizontal field is  $(H/P)_{1/2} = 6.5 \pm 1 \text{ Oe/Torr}$ .

Measurements of the thermomagnetic force were also made in nitric oxide at pressures of 0.15, 0.25, and 0.36 Torr with the magnetic field vertical (parallel to the thermal gradient). These data are shown as a function of  $H/P$  in Fig. 6. Again the normalized force increases along a single curve in the region where the force increases with increasing  $H/P$ . Also, as in the case of  $O_2$ , at the larger values of  $H/P$  there is no universal

curve for these data. The maximum value reached for the normalized force is about  $8 \times 10^{-4} \text{ dyn}/^\circ C$ . The  $(H/P)_{1/2}$  value for NO is roughly 70 Oe/Torr for vertical magnetic field.

The existence of the thermomagnetic force has been verified for  $N_2$  and  $CH_4$ . A detailed investigation of the force effect in these gases was not made because the smaller gyromagnetic ratio for these molecules makes it necessary to go to larger fields than were available.

An attempt was made to determine whether convection currents contributed to the measured thermomagnetic force. A horizontal baffle made of aluminum foil was placed a few millimeters above the sensing disk. With the exception of a 1-cm-diam hole in the center (for the quartz suspension

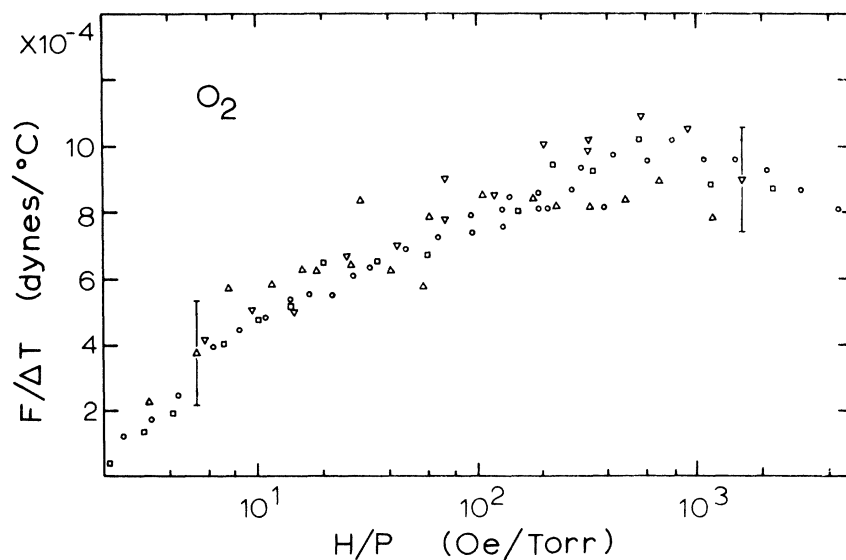


FIG. 4. Thermomagnetic force in  $O_2$  normalized to  $\Delta T = 1^\circ C$  as a function of magnetic field divided by pressure with field parallel to thermal gradient (log scale).  $\circ$ ,  $P = 0.10$  Torr;  $\square$ ,  $P = 0.19$  Torr;  $\nabla$ ,  $P = 0.26$  Torr;  $\Delta$ ,  $P = 0.36$  Torr.

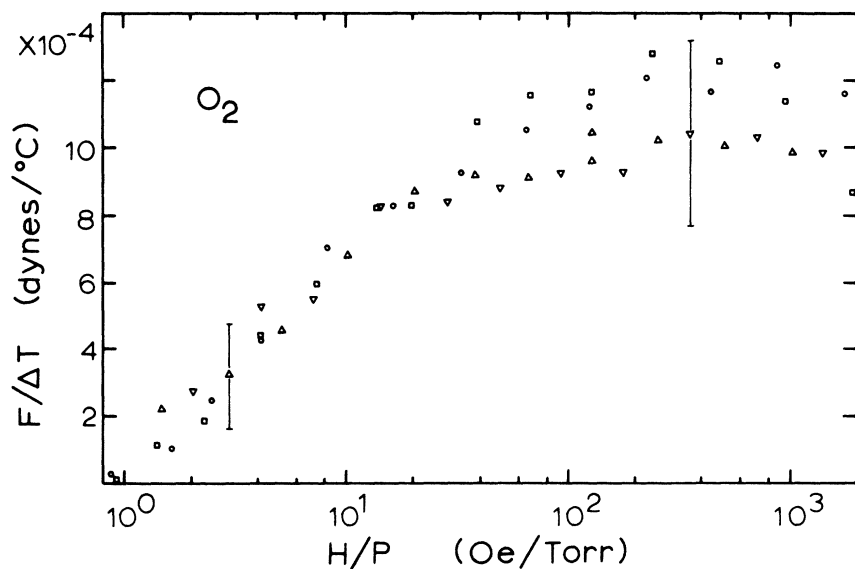


FIG. 5. Thermomagnetic force in  $O_2$  normalized to  $\Delta T = 1^\circ C$  as a function of magnetic field divided by pressure with field perpendicular to thermal gradient (log scale).  $\circ$ ,  $P = 0.10$  Torr;  $\square$ ,  $P = 0.019$  Torr;  $\nabla$ ,  $P = 0.26$  Torr;  $\Delta$ ,  $P = 0.36$  Torr.

fiber), the baffle extended over the whole chamber. Thus any convective flow in the region of the disk would be drastically altered. Thermomagnetic-force measurements made with the baffle in place were identical to those made without it.

#### IV. DISCUSSION OF RESULTS

The thermomagnetic-force effect reported here may be compared to the Senftleben-Beenakker (SB) effect. The force effect approaches a maximum as a universal function of  $H/P$ , as does the SB effect. Both effects increase in magnitude in the same region of  $H/P$ . Figure 7 shows a comparison between these two effects in  $O_2$ . The force curve marked  $F_{||}$  is a best-fit curve through

the data points of Fig. 4. This is for the magnetic field vertical and thus parallel to the thermal gradient. The force curve marked  $F_{\perp}$  is a curve through the data points of Fig. 5, which is for the magnetic field horizontal and thus perpendicular to the thermal gradient. The curves marked  $\lambda_{\perp}$  and  $\lambda_{||}$  are SB curves from Hermans *et al.*<sup>14</sup> for the fractional change in thermal conductivity  $\Delta\lambda/\lambda$  of  $O_2$  with the magnetic field, respectively, perpendicular and parallel to the thermal gradient. All four curves increase from a very small value starting at an  $H/P$  value of one and reach saturation at about  $H/P = 600$  Oe/Torr. The  $(H/P)_{1/2} = 6.5, 9, 10,$  and  $14$  Oe/Torr for  $F_{\perp}, \lambda_{\perp}, F_{||},$  and  $\lambda_{||}$ , respectively. When the magnetic field is

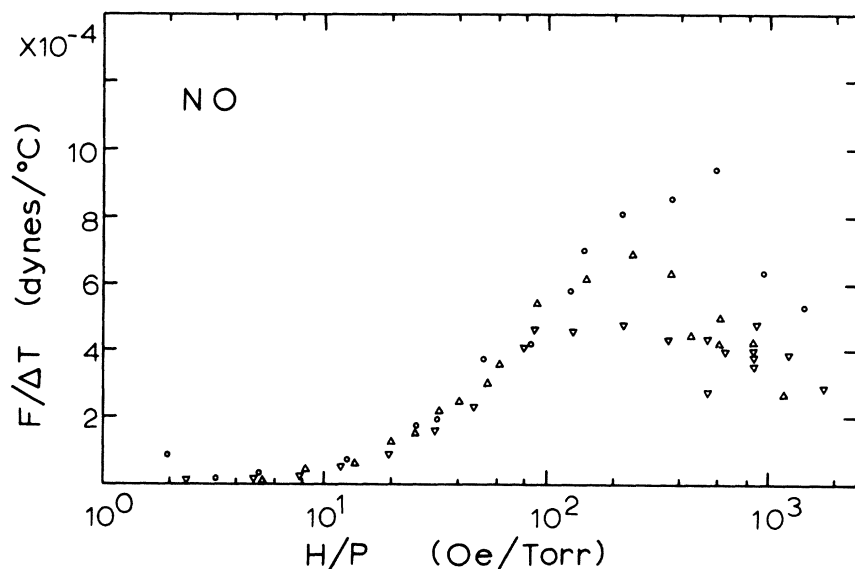


FIG. 6. Thermomagnetic force in  $NO$  normalized to  $\Delta T = 1^\circ C$  as a function of magnetic field divided by pressure with field parallel to thermal gradient (log scale).  $\circ$ ,  $P = 0.15$  Torr;  $\nabla$ ,  $P = 0.25$  Torr;  $\Delta$ ,  $P = 0.36$  Torr.

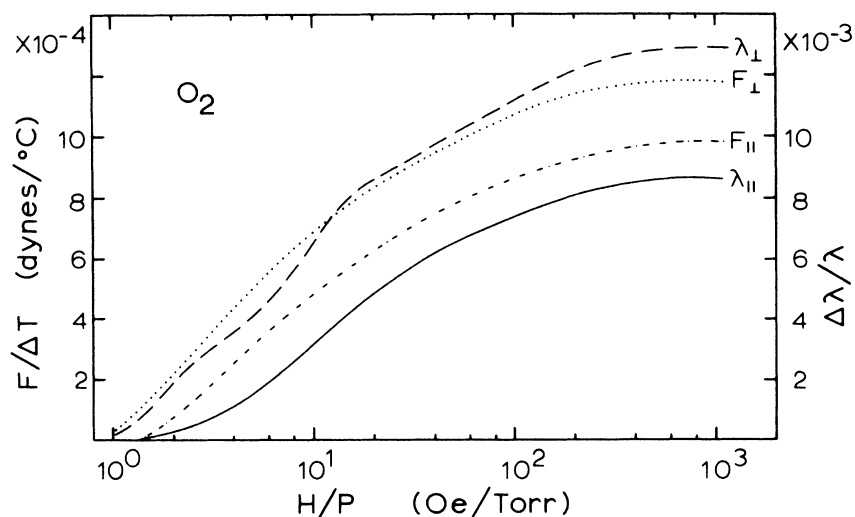


FIG. 7. Thermomagnetic force compared to Senftleben-Beenakker thermal conductivity effect in  $O_2$  (log scale). The scale on the right is the fractional change in thermal conductivity, caused by the field.

changed from the parallel to the perpendicular configuration, both the thermomagnetic-force and the SB-thermal-conductivity effects become larger for given values of  $H/P$ .

A similar comparison can be made for NO. Korving *et al.*<sup>15</sup> have measured the quantity  $\frac{1}{2}(\lambda_{\perp} + \lambda_{\parallel})$  for NO and have obtained  $(H/P)_{1/2} = 53$  Oe/Torr. The value of  $(H/P)_{1/2}$  for  $F_{\parallel}$  from Fig. 6 is approximately 70 Oe/Torr. An exact general value is not possible to obtain because of the difference in the value of the force for the different pressures at the larger  $H/P$  values. Nitric oxide has a larger  $(H/P)_{1/2}$  value than  $O_2$  for both the thermomagnetic-force effect and the SB effect.

A significant difference in the thermomagnetic-force effect and the SB effect occurs at large  $H/P$  values. For the SB effect, both the thermal conductivity and the viscosity reach a saturation value at large enough values of  $H/P$  and may be understood by the mean-free-path change explained by Gorter.<sup>3</sup> The force effect increases with  $H/P$  in much the same way as the SB effect. But it is quite obvious in Fig. 6 that, for NO, as  $H/P$  is increased further the force decreases. For  $O_2$ , the data appear consistent with a saturation-type curve,<sup>16</sup> but a close examination of the data of Fig. 4 and Fig. 5 for each individual pressure makes it apparent that the force decreases as  $H/P$  is increased above about 500 Oe/Torr.

Another difference in the two effects is that the SB effect is a universal function of  $H/P$  for the entire range of values covered. This does not appear to be true in the force effect. For NO, the effect is a function of  $H/P$  up to a value of 100 Oe/Torr. However, above that value the size of the effect depends on the pressure. For  $O_2$ , the effect is a function of  $H/P$  up to a value of about 200 Oe/Torr.

The uncertainty in the measurements for the field vertical are indicated by the error bars of Fig. 4. The major cause for uncertainty is in the determination of the value used for the temperature of the sensing disk. The uncertainty in the data for the field horizontal is larger due to a force that was present even when the chamber contained argon gas. This force was a function of the field and was only present when the coils were placed for the horizontal-field measurements. With the coils in the horizontal configuration any small field gradients would be in a direction that would cause a vertical force on a paramagnetic material. The force present in argon gas is believed to be due to the paramagnetic aluminum disk in such a field gradient.

If one applies the simplest kinetic theory, one obtains an expression for the force per unit area acting on the sensing disk in zero magnetic field:

$$F/A = \frac{4}{3}nk_B\lambda \frac{dT}{dX} . \quad (2)$$

The quantity  $n$  is the number density,  $k_B$  is the Boltzmann constant,  $\lambda$  is the mean free path, and  $dT/dX$  the thermal gradient. This oversimplified equation yields a value for the force per unit area for  $O_2$  which is within a factor of 2 of the measured value from Fig. 2. More complete theories<sup>13</sup> emphasize effects taking place at the edge of the disk.

The Gorter<sup>3</sup> theory for the SB effect indicates that the application of a magnetic field decreases the mean free path. Equation 2 indicates that the force per unit area on the disk is a function of the mean free path. Therefore, the application of a magnetic field in the thermomagnetic-force experiment would be expected to decrease the mean free path and therefore decrease the force pushing the disk away from the hot plate. Our experiments show that this is what happens.

The above theory assumes that the thermomagnetic-force effect is an effect over the area of the disk rather than an edge effect. This last statement needs experimental verification and a new apparatus is presently being built which will allow measurements to be made on a number of different size disks with varying edge-to-area ratios. We hope to show conclusively whether our new results are a surface effect or an edge effect.

The exact molecular-collision mechanism giving

rise to the thermomagnetic force is not known and theoretical calculations have not yet been reported. We conclude that the thermomagnetic force is closely related to the SB effect. It is hoped that the work reported here on the force effect will contribute to a better understanding of the molecular interactions in polyatomic gases and also to a better understanding of how these molecular interactions are reflected in the transport properties.

\*Research supported by The Robert A. Welch Foundation, Houston, Tex.

†Present address: Stout State University, Menomonie, Wisc. 54751.

<sup>1</sup>H. Senftleben, *Z. Physik* **31**, 822 (1930); **31**, 961 (1930).

<sup>2</sup>H. Engelhardt and H. Sack, *Z. Physik* **33**, 724 (1932).

<sup>3</sup>C. J. Gorter, *Naturwiss.* **26**, 140 (1938).

<sup>4</sup>F. Zernike and C. Van Lier, *Physica* **6**, 961 (1939).

<sup>5</sup>J. J. M. Beenakker, G. Scoles, H. F. P. Knaap, and R. M. Jonkman, *Phys. Letters* **2**, 5 (1962).

<sup>6</sup>J. J. M. Beenakker, *Festkörperprobleme* **8**, 275 (1968).

<sup>7</sup>J. J. M. Beenakker and F. R. McCourt, *Ann. Rev. Phys. Chem.* **21**, 47 (1970).

<sup>8</sup>G. G. Scott, H. W. Sturmer, and R. M. Williamson, *Phys. Rev.* **158**, 117 (1967).

<sup>9</sup>D. A. Avery and T. W. Adair, III, *Phys. Rev.* **188**, 512 (1969).

<sup>10</sup>D. H. Weinstein and J. Keeney, *Phys. Rev. Letters* **23**, 218 (1969).

<sup>11</sup>G. G. Scott, H. W. Sturmer, and M. E. Larchez, *Phys. Rev. A* **2**, 792 (1970).

<sup>12</sup>S. Dushman, *Scientific Foundations of Vacuum Technique* (Wiley, New York, 1949), p. 311.

<sup>13</sup>L. B. Loeb, *The Kinetic Theory of Gases* (McGraw-Hill, New York, 1934), p. 364.

<sup>14</sup>L. J. F. Hermans, J. M. Koks, A. F. Hengeveld, and H. F. P. Knaap, *Physica* **50**, 410 (1970).

<sup>15</sup>J. Korving, W. I. Honeywell, T. K. Bose, and J. J. M. Beenakker, *Physica* **36**, 198 (1967).

<sup>16</sup>M. E. Larchez and T. W. Adair, III, *Phys. Rev. Letters* **25**, 21 (1970).

### Third Sound in Superfluid Helium Films of Arbitrary Thickness\*

David J. Bergman†

*Department of Physics and Astronomy, Tel-Aviv University, Tel Aviv, Israel  
and Soreq Nuclear Research Center, Yavne, Israel*

(Received 3 November 1970)

The hydrodynamic equations of a superfluid helium film are solved numerically to yield the dispersion equation of third sound over a wide range of thicknesses, including both unsaturated and saturated films. An analytical approximation to the dispersion equation is found that is good for the entire range where the equations are valid, and which becomes particularly simple in the case of either very thin or very thick films. A clear physical picture is formed of the processes determining the properties of third sound in thick helium films.

#### I. INTRODUCTION

In a previous article,<sup>1</sup> which will henceforth be referred to as I, we obtained a full linearized hydrodynamic description of the lateral motion that is possible in a thin superfluid film situated upon a flat solid substrate and in equilibrium with its own vapor. The equations obtained there were solved explicitly to determine the dispersion equation for third-sound waves only in the limiting case when

$$\kappa_g \omega / \rho_g C_{pg} c_3^2 \ll 1, \quad \eta_g \omega / \rho_g c_3^2 \ll 1,$$

which means, in practice, very thin films and low

frequencies.<sup>1</sup>

Although this case includes all the third-sound experiments conducted on unsaturated helium films by Rudnick's group at UCLA,<sup>2,3</sup> it is also of interest to solve the equations outside this regime. Atkins's original pioneering experiments to detect third sound and measure its properties were in fact made on saturated helium films<sup>4</sup> (i. e., adsorbed films that form upon the walls of a vessel containing liquid helium, at a height of no more than several centimeters above the surface of the liquid), which are considered to be thick films in the context of this article, and he has published some data on both the velocity and the attenuation of third sound in such